Observed change and the extent of coherence in the Gulf Stream system

Helene Asbjørnsen[1,2], Tor Eldevik[1,2], Johanne Skrefsrud[1,2], Helen L. Johnson[3], and Alejandra Sanchez-Franks[4]

[1]Geophysical Institute, University of Bergen, Bergen, Norway
[2]Bjerknes Centre for Climate Research, Bergen, Norway
[3]Department of Earth Sciences, University of Oxford, Oxford, United Kingdom
[4]National Oceanography Centre, Southampton, United Kingdom

Correspondence: Helene Asbjørnsen (h.asbjornsen@uib.no)

Abstract. By transporting warm and salty water poleward, the Gulf Stream system maintains a mild climate in northwestern Europe while also facilitating the dense water formation that feeds the deep ocean. The sensitivity of North Atlantic circulation to future greenhouse gas emissions seen in climate models has prompted an increasing effort to monitor the various ocean circulation components in recent decades. Here, we synthesise available ocean transport measurements from several observational programs in the North Atlantic and Nordic Seas, as well as an ocean state estimate (ECCOv4-r4), for an enhanced understanding of the Gulf Stream and its poleward extensions as an interconnected circulation system. We see limited coherent variability between the records on interannual time scales, highlighting the local oceanic response to atmospheric circulation patterns and variable recirculation time scales within the gyres. On decadal time scales, we find a weakening subtropical circulation between the mid-2000s and mid-2010s, while the inflow and circulation in the Nordic Seas remained stable. Differing decadal trends in the subtropics, subpolar North Atlantic, and Nordic Seas warrant caution in using observational records at a single latitude to infer large-scale circulation change.

1   Introduction

The steady supply of warm Gulf Stream water from the subtropics to subpolar latitudes is crucial for maintaining a mild, maritime climate in northwestern Europe (Kwon et al., 2010; Palter, 2015). Projected slowdown of the North Atlantic circulation as a response to global warming (e.g., Manabe and Stouffer, 1994; Weijer et al., 2020; Sen Gupta et al., 2021) has therefore motivated extensive observational efforts to monitor and understand variability and potential future change (Cunningham et al., 2007; Mercier et al., 2015; Lozier et al., 2017; Østerhus et al., 2019; Rhein et al., 2019). Inferences about large-scale circulation change are typically made based on observing systems measuring circulation strength at carefully selected fixed locations. However, it remains unclear to what extent, and on which time scales, the extended Gulf Stream system should be considered a meridionally coherent circulation system. Here, we use North Atlantic and Nordic Seas ocean transport measurement records to investigate meridional coherence, interannual variability, and potential trends within the Gulf Stream system.
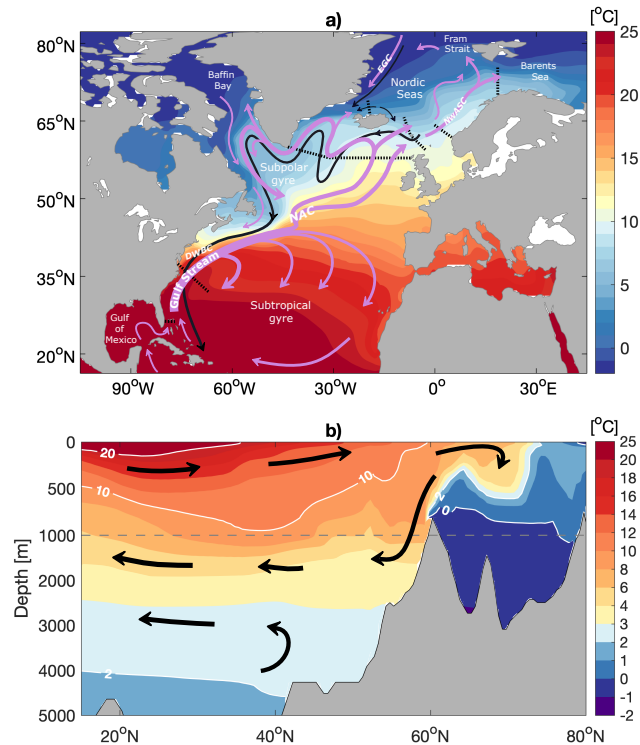
Figure 1. Main North Atlantic and Nordic Seas circulation features. Climatological potential temperature from the ECCOv4 ocean state estimate (1992-2017) with major circulation features indicated in arrows. (a) The horizontal view; purple and black arrows indicate upper-ocean and deep-ocean circulation, respectively (DWBC; Deep Western Boundary Current, NAC; North Atlantic Current, NwASC; Norwegian Atlantic Slope Current, EGC; East Greenland Current). (b) The vertical view; transect follows the WOCE A16 section until 52°N, from where it veers into the Nordic Seas over the Iceland-Scotland Ridge and toward the Fram Strait. In (a) the dashed lines show the observational sections included in the analysis. Note the nonlinear y-axis and nonlinear colorbar in (b).

As a narrow western boundary current, the Gulf Stream is a part of the subtropical gyre (Figure 1a). At approximately 35°N, the Gulf Stream separates from the coast and broadens, reaching a maximum of around 150 Sv at 60°W (Hogg, 1992). The North Atlantic Current continues as the north-eastward extension of the Gulf Stream past the Grand Banks, transporting roughly 27 Sv into the eastern subpolar North Atlantic (Roessler et al., 2015). Substantial subtropical and subpolar recirculation characterizes the North Atlantic circulation (e.g., Daniault et al., 2016). Still, almost 2/3 of the waters flowing across the Greenland-Scotland Ridge into the Nordic Seas come from the Gulf Stream (Asbjørnsen et al., 2021), highlighting the direct connection between the Gulf Stream and the Atlantic water ultimately reaching the Arctic via the Norwegian Atlantic Current. Here, we consider the North Atlantic Current and the Norwegian Atlantic Current as part of the 'Gulf Stream system', but retain the terminology 'the Gulf Stream' for the boundary current along the North American coast.

The Gulf Stream and its poleward extensions are important to the large-scale overturning circulation where water is transformed from light to dense water masses through surface heat loss and mixing at high latitudes (e.g., Mauritzen, 1996; Lozier,

2012). The Atlantic Meridional Overturning Circulation (AMOC) is quantified as the zonally integrated and vertically accumulated meridional flow in the North Atlantic, of which the Gulf Stream and its extensions form the essential northward flowing branch between 25°N and 70°N. The resulting overturning streamfunction depicts an upper-cell where warm, subtropical water flows northward and cold North Atlantic Deep Water flows southward at depth (Figure 1b). While considerable effort has been made to observe and understand the AMOC, it is by definition a zonally integrated view of the circulation which masks variability in the individual currents (e.g., Lozier, 2010; Wunsch and Heimbach, 2013; Roquet and Wunsch, 2022). Both model and observational studies show, for instance, limited coherent variability between subtropical and subpolar AMOC on seasonal to decadal time scales (Bingham et al., 2007; Lozier et al., 2010; Mielke et al., 2013; Moat et al., 2020; Jackson et al., 2022). As an alternative to the integrated AMOC view, we do a first assessment of observed variability in the northward flowing upper-ocean branches within the Gulf Stream system.

The North Atlantic Ocean exhibits pronounced variability on a range of time scales. The dominant mode of interannual atmospheric variability, the North Atlantic Oscillation (NAO; Figure S1), drives ocean circulation changes through both wind stress and surface heat flux anomalies on interannual to decadal time scales (e.g., Eden and Willebrand, 2001; Marshall et al., 2001; Sarafanov, 2009). The subpolar North Atlantic has distinct decadal trends in heat- and freshwater content linked to subpolar gyre dynamics (Piecuch et al., 2017; Desbruyères et al., 2021; Fox et al., 2022). On multidecadal time scales, warm and cold phases referred to as the Atlantic Multidecadal Variability are characterized by basin-wide sea surface temperature anomalies with AMOC variability thought to be an important driver (Zhang et al., 2019). In addition to internal variability, externally forced global warming is projected to slow down the AMOC over the 21st century by reducing dense water formation at subpolar latitudes (e.g., Lique and Thomas, 2018; Weijer et al., 2020).

The observational record is relatively short considering the wide range of time scales characterizing North Atlantic variability. The AMOC strength has been measured in the subtropics at 26.5°N since 2004 (RAPID; Cunningham et al., 2007) and in the subpolar North Atlantic at approximately 55°N since 2014 (OSNAP; Lozier et al., 2017). The Nordic Seas inflow branches and the Norwegian Atlantic Current have been monitored since the 1990s (Orvik and Skagseth, 2003b; Ingvaldsen et al., 2004; Østerhus et al., 2019). For the interannual to decadal time scales resolved by the records so far, it remains unclear to what extent the different branches of the Gulf Stream system will exhibit coherent variability and thus can be used to make inferences about the large-scale circulation. Distinguishing naturally occurring variability from an externally forced global warming signal is furthermore a major challenge (Baehr et al., 2008; Kelson et al., 2022).

Here, we focus on observational records of circulation strength from the Florida Current in the subtropical North Atlantic to the Norwegian Atlantic Current in the Nordic Seas (Figure 2). We use the ECCOv4-r4 ocean state estimate to extend the analysis back to 1992 and explore mechanisms of interannual to decadal variability. In evaluating the Gulf Stream and its poleward extensions as an interconnected circulation system within this time period, we identify patterns of connections and disconnections which have implications for the interpretation of single observational records in the context of large-scale circulation change.

Table 1. Ocean transport measurement records in the North Atlantic and Nordic Seas. The mean transport is the absolute value of the monthly mean volume transport. STD is the standard deviation of the monthly means, with exception of the Oleander record (*) where STD is the standard deviation of annual means. Records included are the Florida Current (FC) and Western Boundary Current (WBC) at RAPID, Gulf Stream (GS) at the Oleander section, North Atlantic Current (NAC) at OSNAP-East, inflow at the Greenland-Scotland Ridge (GSR), and the Norwegian Atlantic Slope Current (NwASC) at Svinøy and the Barents Sea Opening (BSO). Records quantifying overturning strength are included at RAPID (moc_z), OSNAP (moc_σ), and the Greenland-Scotland Ridge (GSR overflow). The notation (moc_z) and (moc_σ) denotes depth-space and density-space overturning strength, respectively.

Section	~Latitude	Time period	Mean [Sv]	STD [Sv]	Data source
RAPID FC	26°N	Mar 1982 - Aug 2021	31.8	2.5	Meinen et al. (2010)
RAPID WBC	26°N	Apr 2004 - Dec. 2020	33.2	3.3	Smeed et al. (2018)
RAPID moc_z	26°N	Apr 2004 - Mar 2020	16.9	3.4	Moat et al. (2020)
Oleander GS	36°N	Jun 1993 - Feb 2018	95.0	4.1*	Rossby et al. (2019)
OSNAP NAC	55°N	Aug 2014 - Jun 2020	19.2	3.2	Fu et al. (2023)
OSNAP moc_σ	55°N	Aug 2014 - Jun 2020	16.4	3.7	Fu et al. (2023)
GSR inflow	60°N	Oct 1994 - Jul 2016	7.4	1.1	Østerhus et al. (2019)
GSR overflow	60°N	Jul 1997 - Apr 2017	5.4	0.5	Østerhus et al. (2019)
Svinøy NwASC	62°N	Apr 1995 - May 2020	4.5	0.9	Orvik (2022)
BSO NwASC	73°N	Sep 1997 - Mar 2017	2.0	1.0	Ingvaldsen et al. (2004)

2 Methods

The strength of the ocean circulation is monitored by a number of observational arrays in the North Atlantic and Nordic Seas. In Section 2.1, we give an overview of the ocean transport measurements used in the analysis (Figure 2): the Florida Current and Western Boundary Current at 26.5°N, the Gulf Stream at the Oleander section, the North Atlantic Current at OSNAP-East, the Greenland-Scotland Ridge inflows to the Nordic Seas, the Norwegian Atlantic Current at Svinøy, and the Atlantic water inflow to the Barents Sea. While our focus is the upper-ocean circulation, we also show estimates of overturning strength (Figure 3): maximum of the overturning streamfunction at the RAPID and OSNAP sections, and overflow transports at the Greenland-Scotland Ridge. The ECCOv4-r4 ocean state estimate is described in Section 2.2, and the data treatment is explained in Section 2.3.

2.1 Observing systems

The Florida Current has been measured since 1982 and is the longest, near-continuous volume transport time series in the North Atlantic (Larsen and Sanford, 1985; Baringer and Larsen, 2001). The volume transport is inferred from submarine telephone cables measuring the motionally induced voltage difference across the strait between Florida and Grand Bahama Island. The 31.8 ± 2.5 Sv transported by the Florida Current constitute the the starting point of the Gulf Stream together with the Antilles
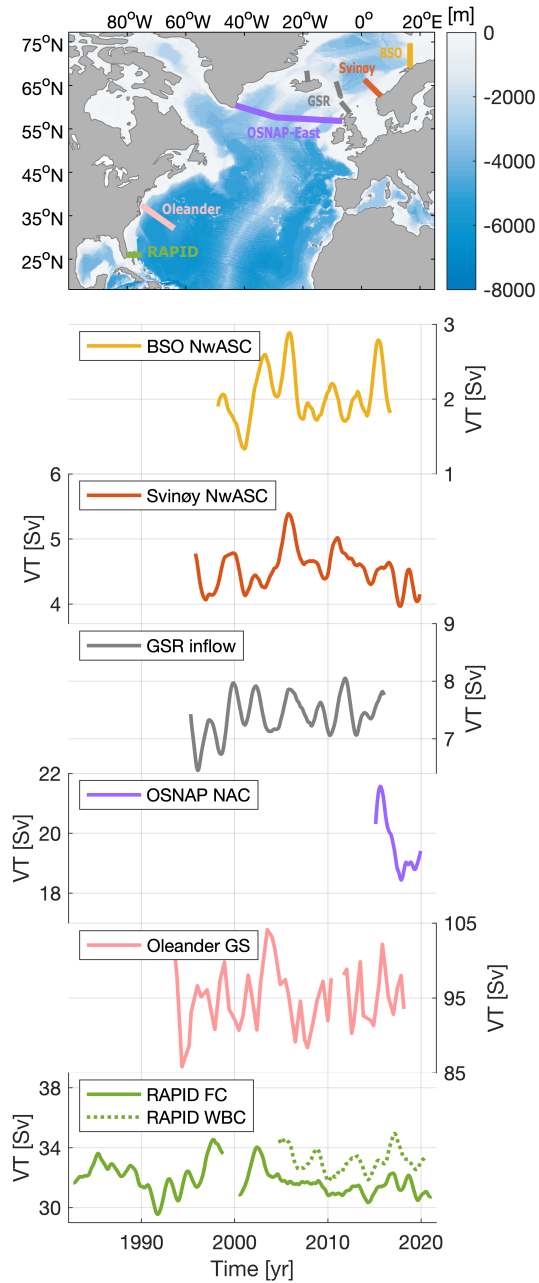
Figure 2. Volume transport time series for the observed Gulf Stream system. From the southernmost to the northernmost section; the Florida Current (FC) and Western Boundary Current (WBC; includes the Antilles Current) at RAPID, the Gulf Stream (GS) component at the Oleander section, the North Atlantic Current (NAC) at OSNAP-East, the combined Faroe-Shetland Channel, Iceland-Faroe-Ridge, and Denmark Strait inflows at the Greenland-Scotland Ridge (GSR), the Norwegian Atlantic Slope Current (NwASC) at Svinøy and at the Barents Sea Opening (BSO). The monthly mean time series have been filtered with a 1-year low-pass triangular filter to highlight interannual variability.

Current to the east (Meinen et al., 2019). Because variability in the Antilles Current is important for the overall variability at the western boundary (Figure 2), we additionally include the total Western Boundary Current transport as defined in Smeed et al. (2018) transporting on average 33.2 ± 3.3 Sv (Table 1).

The RAPID-MOCHA array has been active since 2004, estimating the flow across 26.5°N (Cunningham et al., 2007; Moat et al., 2020). Considering the circulation to be in near geostrophic balance away from boundaries, the RAPID array estimates the mid-ocean geostrophic transport from the thermal wind relation using dynamic height moorings located at the western and eastern continental shelves and on both sides of the Mid-Atlantic Ridge (McCarthy et al., 2015). The full AMOC estimate additionally relies on current meter moorings measuring the Antilles Current, cable measurements from the Florida Current, and the Ekman transport calculated from ERA5 wind stress (Hersbach et al., 2020). The AMOC strength at RAPID shown in Figure 3 is the maximum of the estimated overturning streamfunction in depth-space (moc_z), and thus reflects the strength of the net upper-ocean circulation at 26.5°N.

An ADCP mounted on the container ship $CMV\ Oleander$ allows for estimating volume fluxes from velocities measured along a transect from New Jersey to Bermuda (Flagg et al., 1998; Rossby et al., 2005). The ADCP measures velocities down to 250-400 m depth for the 1992-2004 period, and down to 500-600 m from 2005 and onwards (Sanchez-Franks et al., 2014). Because the measurements do not cover the full depth, the Oleander record is a volume flux for a 1 m thick layer at 52 m depth (unit; Sv/m). We here focus on the Gulf Stream component defined as the northeastward, high-velocity core as provided in Rossby et al. (2019). Using a scale factor of 700, the total Gulf Stream transport in the 0-2000 m layer can be estimated (Rossby et al., 2014), averaging to 95.0 ± 4.1 Sv (Table 1). Due to variable sampling frequency related to ship time and equipment failure, the Oleander transport is estimated in 1-year segments stepped at half-year intervals. As a result, the Oleander record has different temporal resolution than the other time series displayed in Figure 2.

The OSNAP observing system, deployed in 2014, monitors the North Atlantic circulation at subpolar latitudes (Lozier et al., 2017). The two sub-arrays OSNAP-East and OSNAP-West use densely spaced current meter and dynamic height moorings in the boundary currents and over the Reykjanes Ridge. OSNAP also relies on Argo float data, satellite altimetry, glider observations, and the surface wind field to estimate velocities and property fields away from the moorings (Li et al., 2017). Here, we use the North Atlantic Current transport across OSNAP-East (Figure 2), defined as the net transport east of 25.6°W and above the 27.66 kg/m^3 isopycnal. We also show the AMOC strength in density-space (moc_σ) for the full OSNAP line (Figure 3), which quantifies water mass transformation from light to dense water north of the section.

The three inflow branches to the Nordic Seas across the Greenland-Scotland Ridge are monitored by three sub-arrays with current meter moorings at the Faroe-Shetland Channel (Berx et al., 2013), Iceland-Faroe Ridge (Hansen et al., 2015), and north of the Denmark Strait at the Hornbanki section (Jónsson and Valdimarsson, 2012). Regular CTD cruises also sample the sections multiple times a year. For the Faroe-Shetland Channel and Iceland-Faroe Ridge, the volume transport time series combine in situ observations with satellite altimetry. On average, 2.7 ± 1.1 Sv is transported in the Faroe-Shetland Channel, 3.8 ± 0.6 Sv across the Iceland-Faroe Ridge, and 0.9 ± 0.3 Sv with the Denmark Strait branch (Østerhus et al., 2019). While the Iceland-Faroe Ridge component has the highest volume transport of the three inflow branches, the Faroe-Shetland Channel component dominates interannual variability (Figure S2a). In Figure 3, we show the transport of the Greenland-Scotland Ridge
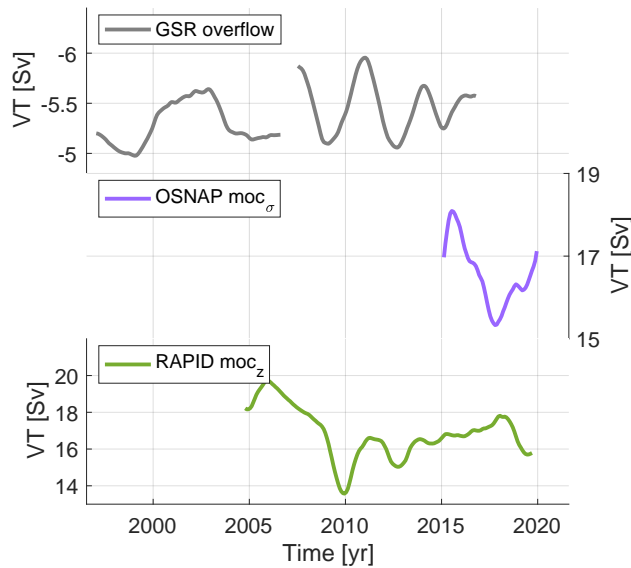
Figure 3. Volume transport time series quantifying overturning strength. The Denmark Strait and Faroe-Bank-Channel overflows at the Greenland-Scotland Ridge (GSR), overturning strength in density space (moc_σ) at OSNAP, and overturning strength in depth-space (moc_z) at RAPID. The monthly mean time series have been filtered with a 1-year low-pass triangular filter to highlight interannual variability. Note that the y-axis of the GSR overflow panel has been flipped.

115 overflows (the Denmark Strait and Faroe-Bank Channel overflows), which quantifies the amount of dense water formed north of the ridge and exported to the Atlantic Ocean (Hansen et al., 2016; Jochumsen et al., 2017).

North of the Greenland-Scotland Ridge, the Norwegian Atlantic Current transports water northward in a two-branch system; the Norwegian Atlantic Slope Current and the Norwegian Atlantic Front Current. A mooring in the Norwegian Atlantic Slope Current has been measuring its variability since 1995 (Orvik and Skagseth, 2003a; Orvik, 2022). The mooring is located at

120 the Svinøy section in the core of the Norwegian Atlantic Slope Current at position 62°48'N, 4°55'E. Because the current is nearly a barotropic shelf edge current, a single current meter at 100 m depth can be used to estimate the total transport of the Norwegian Atlantic Slope Current when scaled with the Svinøy section area (Orvik and Skagseth, 2003a). Applying the scaling factor, the mean Svinøy transport is 4.5 ± 0.9 Sv (Table 1).

At the entrance to the Barents Sea, a current meter mooring array has monitored the Atlantic inflow through the Barents

125 Sea Opening since 1997 (Ingvaldsen et al., 2002, 2004). The mooring array extends from 71°30'N to 73°30'N, with the exact number of moorings deployed varying over the measurement period. On average, the Atlantic inflow through the Barents Sea Opening is 2 ± 1.0 Sv (Table 1).

2.2 ECCOv4-r4 ocean state estimate

To supplement relatively short observational records, we analyse circulation strength in the ECCO Version 4 Release 4
(ECCOv4-r4) ocean state estimate spanning 1992-2017. The ECCOv4-r4 estimate provides a dynamically consistent solution
for the global ocean and sea ice state by using nearly all modern ocean observations to constrain an ocean general circulation
model with a 1° nominal horizontal resolution (Forget et al., 2015; ECCO Consortium et al., 2021). The ECCOv4-framework
uses the adjoint method to iteratively reduce the model-data misfit by adjusting initial conditions, surface boundary conditions,
and model parameters (Heimbach et al., 2005). The observational constraints consist of profiles from Argo floats, Ice-Tethered
Profilers, marine mammals, individual CTD stations, as well as satellite observations of sea level, sea surface salinity and tem-
perature, sea ice concentration, and ocean bottom pressure from GRACE and GRACE-FO. As observed ocean transport time
series are not used as direct constraints in the ECCOv4-framework, the observed and ECCOv4-r4 transport estimates shown
here can be considered independent.

In defining the transport sections in ECCOv4-r4, we stay as geographically close to the observational transects as the coarse
grid allows. For instance, because the complex topography in the Straits of Florida is not fully resolved, we define the Florida
Current transport in ECCOv4-r4 as the transport on the continental shelf. For the full Western Boundary Current transport, the
secondary core with northward flowing water off the shelf is additionally included. We use the same definitions of the currents
as for the observational transports, given that these remain meaningful definitions when studying the ECCOv4-r4 transects. For
instance at OSNAP-East, the same $27.66 \ kg/m^3$ isopycnal is used to define the North Atlantic Current in observations and in
ECCOv4-r4 as watermass properties are generally well-constrained in ECCOv4-r4.

Previous releases of the ECCOv4 state estimate have been shown to reproduce well the observed variability in heat and salt
in the subpolar North Atlantic (Piecuch et al., 2017; Sanders et al., 2022) and the Nordic Seas (Asbjørnsen et al., 2019; Tesdal
and Haine, 2020). In terms of overturning in the North Atlantic, ECCOv4 skilfully reproduces variability at 26.5°N (Evans
et al., 2017; Kostov et al., 2021), though the mean AMOC strength is slightly weaker than in observations (Figure S3). At the
OSNAP-East section, the AMOC strength (here in density-space) is also somewhat weaker than in observations (Figure S4).
ECCOv4-r4 captures the observed peak in moc_σ in 2015/16 (Figure S4c), but the overlapping time period with observations is
too short to get a fair assessment of how well interannual variability is represented.

For the upper-ocean components, interannual variability in the Florida Current is very well represented in ECCOv4-r4
(Figure 4a), though the transport magnitude is slightly lower than in observations (27 Sv versus 32 Sv in observations). At the
Oleander section, direct comparison in terms of variability is difficult due to the temporal resolution of the Oleander record.
However, we note that the Gulf Stream in ECCOv4-r4 fails to intensify sufficiently when moving northward, leaving it too weak
at the Gulf Stream separation latitude - a common issue for ocean and climate models (Sen Gupta et al., 2021). The ECCOv4-r4
estimate captures the volume transport magnitude and variability at the Greenland-Scotland Ridge and Svinøy sections well
(Figure 4a). However, the Greenland-Scotland Ridge inflow in ECCOv4-r4 has a too weak Denmark Strait component (0.2
Sv) and too strong Iceland-Faroe Ridge component (4.7 Sv) compared to observations (0.9 Sv and 3.8 Sv, respectively). The

climatological mean for the Barents Sea Opening inflow is accurate in ECCOv4-r4 (2.03 Sv in observations vs. 2.16 Sv in ECCOv4-r4), though there is little agreement on interannual variability as discussed previously in Asbjørnsen et al. (2019).

2.3 Data treatment

For the observational records with a higher-than-monthly temporal frequency, we compute monthly means of the volume transport time series. To highlight interannual variability, we filter with a 1-year low-pass triangular filter (24-month filter width; Figure 2). Six months are removed at the start and the end of the filtered transport time series to limit the edge effects from filtering. When filtering, shorter gaps in the measurement records (no more than five consecutive months) are smoothed over, while more extensive gaps such as the one between November 1998 and May 2000 in the Florida Current record, are treated as a discontinuous time series. The filtered volume transport anomalies from the time mean are shown when comparing observations and the ECCOv4-r4 state estimate (Figure 4). Because the Oleander transport is estimated in 1-year segments stepped at half-year intervals, it is not low-pass filtered like the other time series.

To assess the co-variability between the transport time series, we calculate the correlation coefficient between the different low-pass filtered observational and ECCOv4-r4 time series. We show correlation at lag zero (Table 2), and for the ECCOv4-r4 estimate we also identify the maximum correlation for lag times between zero and six years (Figure S5). Several of the observational time series have a limited overlapping period of available data, and autocorrelation further limits the number of independent data points. We therefore use the Chelton (1983) method at the 95% confidence level to assess whether the correlation between two time series is significant. The method uses the effective degrees of freedom to compute a correlation coefficient value as a threshold for significance. The threshold for significant correlation varies substantially, taking a high value when the effective degrees of freedom is low. Throughout, we refer to the correlation analysis between the transport sections as a way to assess meridional coherence within the Gulf Stream system.

We estimate linear trends over the extent of the individual observational records using the least squares method (Table 3). Trends in the ECCOv4-r4 state estimate are evaluated over the 1992-2017 period. The trend calculations are performed on the unfiltered monthly mean time series. To assess whether the trend values are significantly different from zero at the 95% confidence level, we use the modified Mann-Kendall test for autocorrelated data (Hamed and Rao, 1997). In Figure S6, we additionally show the 95% confidence interval for the trend estimates.

3 Observed coherence, variability, and change

Observations of circulation strength at fixed locations are often used to make inferences about the state of the large-scale circulation (e.g. Smeed et al., 2018; Østerhus et al., 2019). Here, we view the different circulation components in the context of the extended Gulf Stream system, focusing on observed coherence between the branches monitored on interannual time scales, and potential trends over the respective measurement periods.
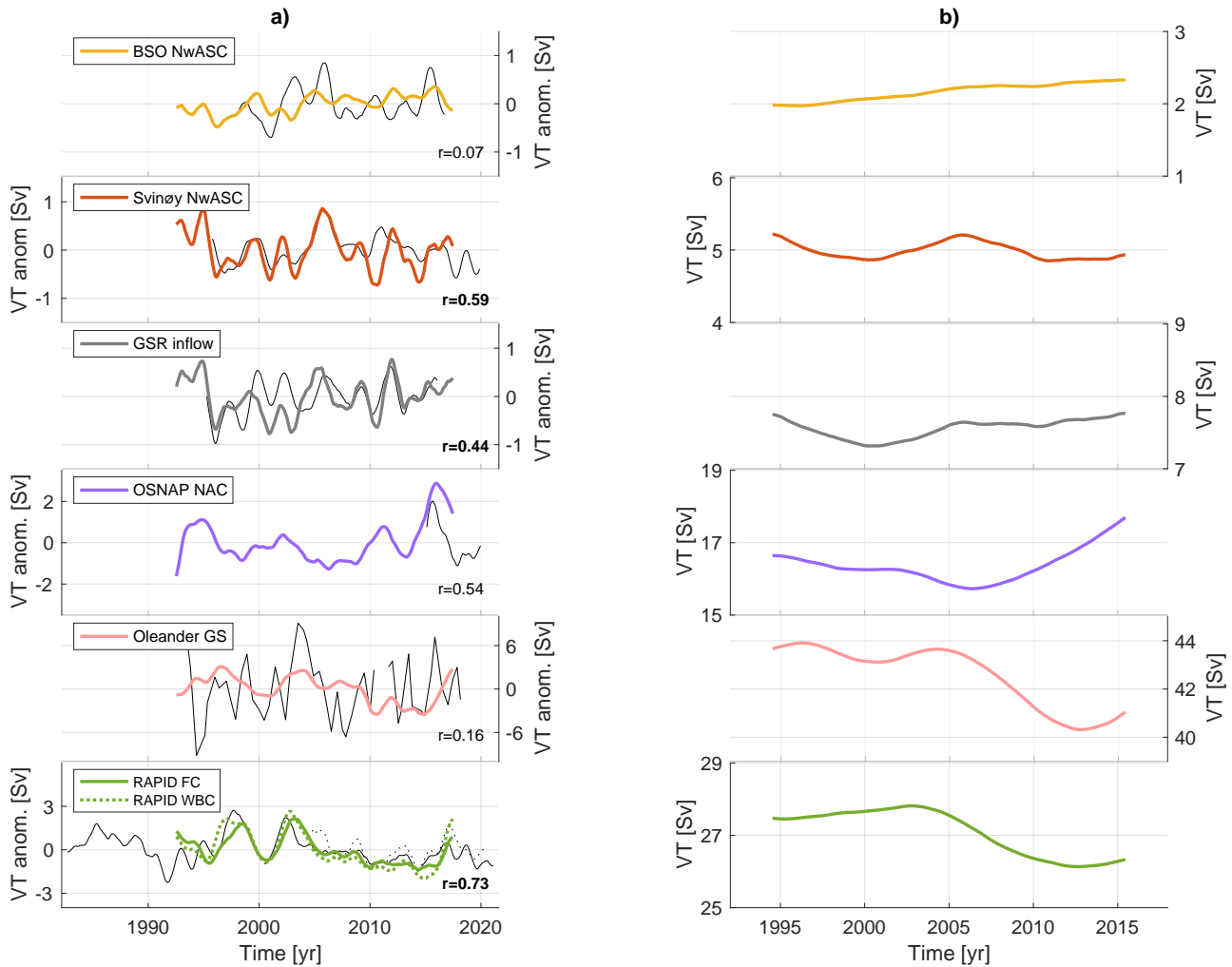
Figure 4. Interannual to decadal volume transport variability in ECCOv4-r4 and observations. (a) ECCOv4-r4 transport anomalies from the time mean (1992-2017) are displayed in colors, with corresponding observational time series (as in Figure 2) in black. Significant correlations between observational and ECCOv4-r4 time series are indicated in bold font. (b) Equivalent ECCOv4-r4 transport sections as in (a), but smoothed with a 5-year low-pass filter to highlight decadal variability. The time series show the total volume transport, not anomalies, so that the magnitude of decadal trends is visible.

3.1 Meridional coherence

Circulation in the North Atlantic Ocean adjusts to changes in local surface forcing (wind and buoyancy) through rapid propagation of boundary waves at the western boundary, slow westward propagation of Rossby waves, and advection of density anomalies with the ocean currents (Johnson and Marshall, 2002; Zhang, 2010; Marshall and Johnson, 2013). The range in time scales of these processes communicating change (advection; ~3-4 years from subpolar to subtropical latitudes, Kelvin waves; < 1 year, Rossby waves; interannual-decadal time scales) makes the adjustment period potentially long, and the system's meridional coherence is thought to increase with increasing time scale considered (e.g., Gu et al., 2020). Limited meridional coherence between the subtropical and subpolar AMOC strength is seen in both models and observations (e.g., Bingham et al., 2007; Lozier et al., 2010; Mielke et al., 2013; Jackson et al., 2022). On interannual time scales, variability in subtropical AMOC strength is dominated by local wind stress, which in-part explains the limited coherence with subpolar AMOC variability driven by a combination of wind and buoyancy anomalies (Zhao and Johns, 2014; Kostov et al., 2021).

More meridionally coherent signals in the AMOC have been explored in previous studies. Using EOF analysis, Zou et al. (2020) identify a meridionally coherent AMOC mode and a gyre-opposing AMOC mode in multiple ocean models. Han (2023) finds a coherent signal on seasonal to interannual time scales in ECCOv4-r3 linked to isopycnal heaving and the associated adiabatic redistribution of water (also called 'sloshing'). Still, the lack of coherence in the full signal remains a challenge for the observing systems and detection of potential emerging trends in the North Atlantic circulation (Frajka-Williams et al., 2023).

Comparing the volume transport time series of the upper-ocean branches included in our analysis shows limited meridional coherence within the Gulf Stream system on interannual time scales for all sensible lags (Table 2, Figure S5a). The North Atlantic Current at the OSNAP-East section shows high zero-lag correlation with the Greenland-Scotland Ridge, Svinøy, and Barents Sea Opening sections downstream, but the correlations are not statistically significant as the degrees of freedom are low for the short OSNAP record (Table 2). Between the transport at the Svinøy section and the inflow through the Barents Sea Opening, there is a weak but statistically significant relationship (r=0.30) at zero lag time. The remaining observational records show little sign of covariance. For instance, the correlation between the Western Boundary Current at 26.5^oN and the Gulf Stream at Oleander is not significant, which is consistent with previous studies finding surface-layer transport to decorrelate quickly when moving north along the Gulf Stream path (Chi et al., 2023).

In contrast to the observational records, some more distinct patterns of coherence are found within the ECCOv4-r4 estimate (Table 2). The strongest relationships identified are at zero lag time between transport sections that are geographically close and upstream of major recirculation branches. Specifically, we find coherence within the Gulf Stream boundary current (Florida Current/Western Boundary Current at 26.5^oN and the Oleander section) and within the Nordic Seas (Greenland-Scotland Ridge inflow, Svinøy, Barents Sea Opening). Covariability at zero lag must be a result of fast boundary wave propagation or the ocean responding to regional scale atmospheric forcing. Testing for a range of lag times, we find no covariance between the subtropics and the subpolar North Atlantic, or the subpolar North Atlantic and the Nordic Seas on interannual time scales in ECCOv4-r4 (Figure S5a).

Table 2. Correlation between the transport sections. Correlations at zero lag time between low-pass filtered volume transport anomalies from the time mean for the observational records (gray cells; see Table 1 for overlapping time periods), and for the equivalent ECCOv4-r4 transport (white cells; 1992-2017 period). For the Oleander observational record, linear interpolation is used to obtain monthly values for the correlation. Significant correlations at the 95% confidence level are in bold font (Chelton (1983) method for evaluating significance).

	RAPID FC	RAPID WBC	Oleander GS	OSNAP NAC	GSR inflow	Svinøy NwASC	BSO NwASC
RAPID FC	1	**0.71**	0.07	0.08	-0.16	-0.25	0.22
RAPID WBC	**0.91**	1	0.26	-0.16	0.21	0.15	0.25
Oleander GS	**0.71**	**0.78**	1	0.43	-0.15	-0.12	0.36
OSNAP NAC	-0.27	-0.20	-0.19	1	0.82	0.73	0.88
GSR inflow	-0.12	-0.27	-0.06	0.18	1	0.38	0.10
Svinøy NwASC	0.06	-0.05	0.19	-0.00	**0.79**	1	**0.30**
BSO NwASC	-0.46	**-0.63**	-0.54	0.09	**0.52**	**0.32**	1

Within the Ekman layer, the ocean responds to the local surface wind stress independently at each latitude. We therefore additionally check coherence within ECCOv4-r4 when removing the upper 100m before integrating across the sections (Table S1). Removing the Ekman layer does not notably increase the correlations or establish any new relationships between the analysed sections. Similarly to the full section transports, testing for different lag times reveals no systematic patterns of coherence that can be linked to advection times of anomalies (Figure S5b).

Based on the correlations between the ECCOv4-r4 transport sections, we conclude that meridional coherence in the Gulf Stream system is limited to the gyre structures on interannual time scales, considering the Nordic Seas boundary current system as a separate gyre-like structure. We see, similarly, that the three main gyres structures exhibit differing behaviour also on decadal time scales (Figure 4b), which is discussed further in Section 3.2.

3.2 Change over the observational record

Under future emission scenarios, climate models consistently project a weakened AMOC (e.g., Weijer et al., 2020) and to somewhat lesser extent, Gulf Stream (Sen Gupta et al., 2021; Asbjørnsen and Årthun, 2023). There is, however, no consensus on whether such a weakening has already occurred over the past century. Some paleo and proxy reconstructions indicate that the AMOC has already weakened (e.g., Thornalley et al., 2018; Caesar et al., 2021), potentially by as much as 15% since the mid-20th century (Caesar et al., 2018). Kilbourne et al. (2022) argue, on the other hand, that circulation strength from paleo records is poorly constrained, and advise against concluding from subsets of records. When a more complete set of available proxy records for the AMOC is considered the findings are inconclusive (Moffa-Sánchez et al., 2019), illustrating the complex relationship between the ocean state and the different proxy types and locations.

Various methods to reconstruct the circulation strength from historical hydrography or sea level are commonly applied as an alternative to paleo proxies for the most recent century. Fraser and Cunningham (2021) find no statistically significant trend over

Table 3. Linear trends over monthly mean transport time series in observations and in ECCOv4-r4 (1992-2017). The trends are given in Sv/year. For the observations, the time periods over which the trends are calculated are given in Table 1. Significant trends at the 95% confidence level in bold font (modified Mann-Kendall trend test for autocorrelated data (Hamed and Rao, 1997)). The 95% confidence intervals for the estimated trends are shown in Figure S6.

Trends in:	Observations	ECCOv4-r4
RAPID FC	**-0.030**	**-0.067**
RAPID WBC	-0.036	**-0.074**
Oleander GS	0.022	**-0.108**
OSNAP NAC	-0.160	**0.052**
GSR inflow	**0.012**	0.006
Svinøy NwASC	-0.002	-0.012
BSO NwASC	0.011	**0.015**

the past century (1900-2019) when using the Bernoulli inverse to reconstruct the AMOC strength from hydrography at 50°N.
245 Similarly, Rossby et al. (2020) find no long-term trend (1900-2020) in the reconstructed geostrophic transport of the Nordic Seas inflow, or in the Gulf Stream volume transport from direct observations (Rossby et al., 2014). Using inverse models based on hydrographic transects, Caínzos et al. (2022) find no systematic change in the AMOC at any latitude when comparing the past three decades; neither do Fu et al. (2020). Reconstructing the AMOC at 26°N for the 1981-2016 period from hydrography, Worthington et al. (2021) similarly find no decline in the subtropical AMOC. At the same latitude, Piecuch (2020) finds some
250 indication of a weakening Florida Current over the 1909-2018 period using historical tide gauge measurements and Bayesian analysis. In the observational records analysed here, only the Florida Current and AMOC at RAPID (both at 26°N) display a statistically significant weakening over their respective observational periods (Table 3, Table S2). A weakening Florida Current since 1982 is also found in a recent, more comprehensive analysis, combining the cable measurements with altimetry and in-situ measurements and their associated observational uncertainties (Piecuch and Beal, 2023). For the ECCOv4-r4 period
255 (1992-2017), we find a significant weakening trend for all the subtropical sections (Table 3) due to weakening transports between the mid-2000s and mid-2010s (Figure 4b). We note, however, that the weakening trend identified for the subtropical sections cannot be explicitly connected to anthropogenic forcing. Pronounced multidecadal transport variability is highlighted in previous studies (e.g., Fraser and Cunningham, 2021; Rossby et al., 2020) and the 26-year ECCOv4-r4 period is too short to represent such multidecadal signals. At RAPID, the notable weakening in overturning between 2006 and 2010 is explained
260 by changes in the upper mid-ocean transport and Ekman transport components (Figure S2c), which have been shown to result from adjustments to wind forcing (Roberts et al., 2013; Zhao and Johns, 2014). To detect anthropogenically forced weakening at 26°N, as much as 60 years of observations could be required (Baehr et al., 2008; Lobelle et al., 2020).

In the subpolar North Atlantic, the North Atlantic Current at OSNAP-East displays a strengthening after 2007 consistent with a strengthening subpolar gyre in that period (Koul et al., 2020). At the Greenland-Scotland Ridge and in the Nordic Seas, the

265 circulation shows no weakening over the different observational records or for the ECCOv4-r4 period (Tables 3). As pointed out in Østerhus et al. (2019), the observed overflow transports seen in Figure 3 indicate that any AMOC slowdown during the past two decades does not stem from reduced overturning in the Nordic Seas and Arctic Ocean. North of the Greenland-Scotland Ridge, transports at Svinøy show no trend (Orvik, 2022, and Table 3). At the Barents Sea Opening there is a strengthening over the ECCOv4-r4 period which is not seen in the observational record (Table 3). However, trends in observed sea surface

270 height found in Polyakov et al. (2023) suggest that there might have been an increased transport in the northernmost Barents Sea Opening inflow branch after the mid-2000s that is not fully captured by the mooring array.

Consistent with our results, previous studies have also found differing decadal trends between the subtropical, subpolar, and Nordic Seas gyres. For instance, Jackson et al. (2022) show evidence of differing decadal trends in the subtropical and subpolar AMOC over the historical record. They find a strengthening subtropical AMOC from 2001 to 2005 and a weakening

275 from 2005 to 2014, while the subpolar AMOC likely strengthened from 1980 to the mid-1990s and then weakened until the 2010s. In future emission scenarios, climate models show the Nordic Seas gyre strengthening in the second half of the 21st century, something which enhances water mass transformation in the Nordic Seas and thus may act as a stabilizing factor for an overall weakening AMOC south of the Greenland-Scotland Ridge (Årthun et al., 2023).

3.3   Mechanisms of interannual to decadal variability

280 Variability in the North Atlantic and Nordic Seas is closely linked to atmospheric forcing. To identify the atmospheric circulation patterns most closely associated with interannual volume transport variability at the ocean observation sites, we regress the annual mean sea level pressure onto the annual mean volume transport time series in ECCOv4-r4 (Figure 5, Figure S7) and in observations (Figure S8). Consistent with the analysis assessing meridional coherence (Table 2), we find interannual variability in the subtropics, subpolar North Atlantic, and Nordic Seas to be associated with different atmospheric circulation

285 patterns.

For the subtropical ocean transports, a low-pressure anomaly over the Labrador Sea and a basin-wide high-pressure anomaly over the subtropics are associated with a stronger Gulf Stream on interannual time scales (Figure 5a-b). Previously, Baringer and Larsen (2001) found a negative correlation between the Florida Current strength and the NAO on interannual time scales, but the relationship was only seen to hold for the period 1986-1998 (Meinen et al., 2010; Sanchez-Franks et al., 2014). Rather than

290 the NAO and associated shifts in the latitude and strength of the climatological sea level pressure pattern, Hameed et al. (2021) find a link between the longitudinal position of the Icelandic Low and Florida Current transport at zero lag time ($r = -0.50$). When perturbing the ECCOv4-r4 state estimate with the onshore wind stress anomalies associated with an eastward shifted Icelandic Low, they get a sea level increase along the North American coast and a weakened Florida Current. The pattern seen in Figure 5a-b associated with a strengthened Gulf Stream resembles a westward shift of the Icelandic Low and is thus

295 consistent with the mechanism in Hameed et al. (2021), previously also shown to be important for shifts in the Gulf Stream northern boundary (Sanchez-Franks et al., 2016). However, we note that several mechanisms not addressed here are thought to contribute to interannual variability in the Florida Current, such as eddy activity east of The Bahamas (Frajka-Williams et al., 2013), excursions of the Loop Current upstream (Hirschi et al., 2019), and ENSO (Dong et al., 2022).
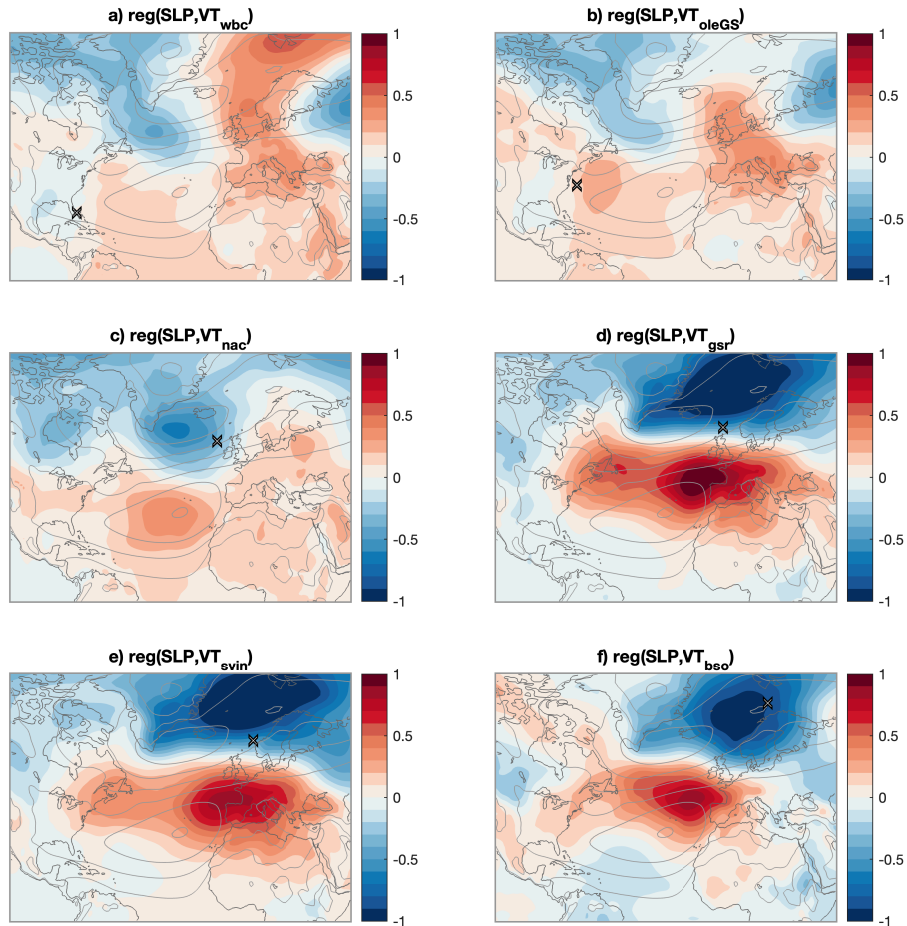
Figure 5. Transport variability and large-scale atmospheric circulation patterns. Annual mean sea level pressure (SLP; hPa) regressed onto annual mean volume transport (VT; Sv) time series in ECCOv4-r4; (a) Western Boundary Current at 26.5^{o}N (wbc), (b) Gulf Stream at the Oleander section (oleGS), (c) North Atlantic Current at OSNAP-East (nac), (d) Greenland-Scotland Ridge inflow (gsr), (e) NwASC at Svinøy (svin) and (f) Barents Sea Opening (bso). The volume transport time series has been normalized $\left(\frac{X-\mu_x}{\sigma_x}\right)$ for comparable magnitudes between the panels. The unit is hPa per standard deviation of volume transport. The major features in the regression patterns discussed are significant at the 90% confidence level (Ebisuzaki, 1997). Gray contour lines show the climatological SLP pattern (contour interval: every 3 hPa from 1007 to 1019 hPa). The crosses mark the approximate location for the volume transport time series.
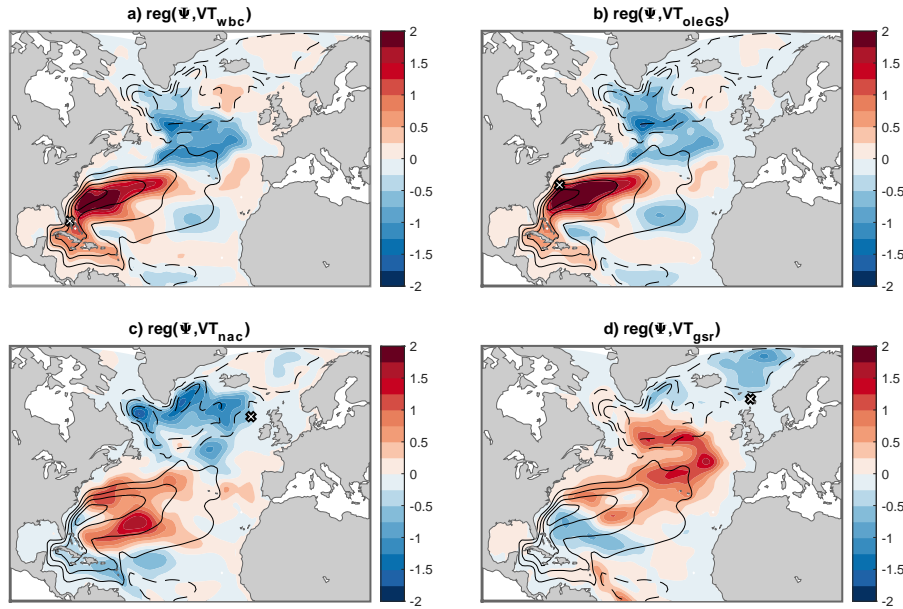
Figure 6. Transport variability and large-scale oceanic circulation patterns. Annual mean barotropic streamfunction (ψ; Sv) regressed onto annual mean volume transport (VT; Sv) time series in ECCOv4-r4; (a) Western Boundary Current at 26.5^{o}N (wbc), (b) Gulf Stream at Oleander section (oleGS), (c) North Atlantic Current at OSNAP-East (nac), (d) Greenland-Scotland Ridge inflow (gsr). The volume transport time series has been normalized ($\frac{X-\mu_x}{\sigma_x}$) for comparable magnitudes between the panels. Unit is Sv per standard deviation of volume transport. Gray contour lines show the climatological barotropic streamfunction pattern (dashed line where ψ takes negative values). The crosses mark the approximate location for the volume transport time series. The major features in the regression patterns discussed are significant at the 90% confidence level (Ebisuzaki, 1997).

For the North Atlantic Current across OSNAP-East, an increased transport is associated with a strengthened climatological
300   sea level pressure pattern resembling the NAO in a positive state (NAO+; Figure 5c). On interannual time scales, the pattern likely relates to locally strengthened westerly winds which strengthen the subpolar gyre as seen in the associated barotropic streamfunction in Figure 6c. In ECCOv4-r4, a strengthened North Atlantic Current across OSNAP-East thus reflects a stronger subpolar gyre, but does not necessarily lead to a strengthened inflow across the Greenland-Scotland Ridge or a strengthened Nordic Seas gyre. The finding is consistent with the weak correlations between the North Atlantic Current and the downstream
305   components in Table 2. The decadal trends in the North Atlantic Current (Figure 4b) agree with multiple subpolar gyre indices indicating a weakening subpolar gyre from the mid-1990s to 2005, followed by a strengthening (Koul et al., 2020). The evolution fits with the accumulated historic NAO forcing seen in Figure S9, consistent with persistent NAO+ conditions spinning up the subpolar gyre due to strengthened wind stress curl and elevated heat loss (Eden and Willebrand, 2001; Sarafanov, 2009).

The sea level pressure pattern associated with a strong Greenland-Scotland Ridge inflow (Figure 5d) mainly arises from the
310   Faroe-Shetland Channel component which dominates the net inflow variability (Figure S2a). The pattern in Figure 5d shows a strengthened and northeastward shifted Icelandic low and Azores high, which is near identical to the equivalent regressions

for the Svinøy and Barents Sea Opening sections (Figure 5e-f). The northeastward shift suggests a corresponding shift of the westerlies and the storm tracks. From previous studies it is well established that the Faroe-Shetland Channel inflow typically increases under NAO+ conditions due to a strengthened sea surface height gradient across the channel (e.g. Chafik, 2012;

315 Bringedal et al., 2018). Regressing ERA5 sea level pressure onto the observational Faroe-Shetland Channel volume transport shows a more canonical NAO+ anomaly consistent with previous studies (not shown). For variability at the Svinøy section, the relationship with the NAO is less straightforward and known to be more closely associated with the position of the westerlies rather than the strength (Orvik, 2022). More low-pressure systems directed into the Nordic Seas due to a northeastward shifted storm track strengthen the southwesterly winds along the Norwegian coast, and sets up onshore Ekman transport and piling

320 along the coast which in turn strengthens the Norwegian Atlantic Slope Current (Skagseth and Orvik, 2002; Richter et al., 2009). The barotropic streamfunction anomaly associated with a stronger Greenland-Scotland Ridge inflow (and Svinøy and Barents Sea Opening components) is a strengthened Nordic Seas gyre (Figure 6d). Moreover, the anticyclonic anomaly in the intergyre-region seen in Figure 6d can be interpreted as a more tilted North Atlantic Current (Marshall et al., 2001), which potentially means that more water crosses the Greenland-Scotland Ridge and less recirculates within the subpolar gyre.

325 We do find relatively straightforward relationships between regional atmospheric circulation (represented by sea level pressure) and the section volume transports. These zero-lag regressions (Figure 5) are likely most representative of sea level pressure patterns related to ocean circulation's relative immediate barotropic response to anomalous atmospheric forcing (e.g., Eden and Willebrand, 2001). It should be noted that the ocean responds to the atmosphere on a range of time scales and also influences the atmosphere through feedback mechanisms (Marshall et al., 2001).

330 The barotropic streamfunction anomaly patterns (Figure 6) indicate that strong transports at the individual sections are typically associated with a strengthened gyre structure locally, with little sign of the other two gyres strengthening simultaneously. This suggests that recirculation and branching within the three major gyres is likely a key factor in explaining the lack of coherence between the northward transport within each gyre structure. For instance, downstream of the 95 Sv in the Gulf Stream core at Oleander, substantial subtropical recirculation occurs (Mann, 1967; Meinen and Watts, 2000) as well as mixing with

335 subpolar water masses (e.g., Brambilla et al., 2008) before the North Atlantic Current transports roughly 20 Sv across OSNAP-East. Of the 20 Sv crossing OSNAP-East, only 7-8 Sv crosses the Greenland-Scotland Ridge meaning that roughly 50% of the water recirculates within the subpolar gyre (Table 1). Our results thus indicate that while the subtropical gyre, subpolar gyre, and Nordic Seas gyre are connected through the northward transport of subtropical-origin water, they are disconnected by the recirculation within the gyres (Figure 7).

4 Summary and conclusions

In this study, we have synthesized available ocean transport measurements and the ECCOv4-r4 ocean state estimate to investigate variability within the Gulf Stream system on interannual to decadal time scales. We find little coherence between the observational records at different latitudes on interannual time scales (Table 2). In the ECCOv4-r4 estimate we find evidence of regional coherence, with subtropical variability being distinct from subpolar and Nordic Seas variability. These findings also
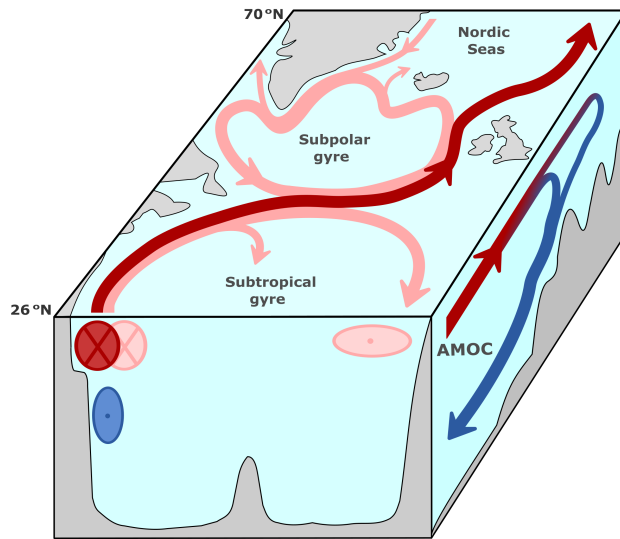
Figure 7. Idealized view of the North Atlantic and Nordic Seas circulation. The Gulf Stream system is connected through the northward transport of subtropical-origin water (red color), but disconnected by recirculation within the gyre structures (pink color). Seen from a mass-balance perspective at 26°N, the Gulf Stream is shown using two circles highlighting it partly compensating for the Deep Western Boundary Current and partly being the western boundary of the wind-driven subtropical gyre. The Deep Western Boundary Current flowing south is represented by the blue circle at depth. The zonally-integrated view of the circulation is shown on the side, illustrating warm upper-ocean water being gradually transformed and sinking at high latitudes as a part of the AMOC.

345   translate to decadal time scales, where in ECCOv4-r4 we find a weakening Florida Current at 26.5^{o}N and Gulf Stream at the Oleander section after the mid-2000s, while the Nordic Seas inflow and circulation remain stable or strengthened (Table 3, Figure 4b).

    A higher degree of coherence within the ECCOv4-r4 framework compared to the observational records can be due to a number of reasons. Firstly, the overlapping time periods between some of the observational records are short, making the
350   threshold for significance high. Secondly, ECCOv4-r4 has a coarse model grid which will smooth high-frequency variability from, for instance, eddies. Thirdly, just as models have their biases, observational records have observation errors related to calibration, sampling, and system design (e.g., McCarthy et al., 2015) which potentially could hide a more meridionally coherent signal.

    The limited coherence across the subtropical, subpolar, and Nordic Seas gyres identified here highlights the role of local
355   oceanic response to atmospheric circulation patterns. Specifically, transport variability within the gyres is associated with variability in the position and strength of the Azores high and the Icelandic low (Figure 5), meaning that regional atmospheric circulation patterns are a major influence at the observation locations through strengthening or weakening the different gyres. Removing the Ekman layer transports from the analysis does not notably increase covariance between the sections on inter-annual time scales (Table S1), meaning that it is not simply transport anomalies in the Ekman layer that overshadow a more

meridionally coherent signal. While we focus on upper-ocean transports in the Gulf Stream system, our findings agree with observed (Lozier et al., 2010; Frajka-Williams et al., 2019; Moat et al., 2020; Jackson et al., 2022) and simulated (Bingham et al., 2007; Gu et al., 2020) patterns of disconnect between the subpolar and subtropical AMOC, highlighting different overturning behaviours between the gyres (Figure 7).

While observations and models show that ocean heat anomalies and other tracers can propagate persistently poleward through the North Atlantic Ocean, leading to potential for skillful climate prediction (e.g., Keenlyside et al., 2008; Årthun et al., 2017), our results herein indicate that volume transport anomalies do not. Therefore, the mechanism by which the gyres exchange, for instance, heat anomalies, remains unclear and is thus a challenge to address following up on the present study.

In climate models, the Gulf Stream is projected to weaken over the 21st century as both the Deep Western Boundary Current and the subtropical gyre circulation weakens (Beadling et al., 2018; Asbjørnsen and Årthun, 2023). Being limited to interannual-decadal time scales, we are unable to determine how the observational trends over the respective measurement periods (Table 3) relate to anthropongenic forcing. We note, however, that none of the circulation branches display any signs of past or near-future collapse. The RAPID record, moreover, shows that sizable shorter term trends such as the reduced overturning between 2006 and 2010 (Figure S2c) can occur from oceanic adjustments to surface wind forcing (Roberts et al., 2013; Zhao and Johns, 2014; Kostov et al., 2021).

In finding little coherence between the gyre structures on interannual to decadal time scales, our results reinforce the need for caution in inferring large-scale circulation change from single observational records within the time scales that are currently resolved. Improved mechanistic understanding of the variability and continued monitoring of the circulation at a range of latitudes is therefore required to predict and detect emerging trends.

Data availability. The ECCOv4-r4 ocean state estimate (ECCO Consortium et al., 2021) is available at https://ecco-group.org/products.htm. ERA5 reanalysis data (Hersbach et al., 2020) is available at https://doi.org/10.24381/cds.f17050d7. Observational Barents Sea Opening and Svinøy volume transport time series (Ingvaldsen et al., 2004; Orvik, 2022) are available through the Norwegian Marine Data Centre (http://metadata.nmdc.no/UserInterface) and are provided by the Institute of Marine Research and University of Bergen, respectively. Greenland-Scotland Ridge volume transports (Østerhus et al., 2019) are available online at http://www.oceansites.org/tma/gsr.html. The OS-NAP observational data (Fu et al., 2023) is available at https://doi.org/10.35090/gatech/70342 through the Overturning in the Subpolar North Atlantic Program. Oleander section volume fluxes (Rossby et al., 2019) are available at https://oleander.bios.asu.edu/data/oleander-fluxes/ through the Oleander Project. The RAPID-MOCHA-WBTS observational data (Moat et al., 2022) is available at https://doi.org/10.5285/e91b10af-6f0a-7fa7-e053-6c86abc05a09 through the RAPID-Meridional Overturning Circulation and Heatflux Array-Western Boundary Time Series programme. The Florida Current volume transports (Meinen et al., 2010) are available on the Atlantic Oceanographic and Meteorological Laboratory web page (www.aoml.noaa.gov/phod/floridacurrent/) through the DOC-NOAA Climate Program Office - Ocean Observing and Monitoring Division.

Author contributions. HA, TE, and HLJ defined the overall research problem and methodology. HA carried out the analysis and led the writing of the manuscript. JS developed the conceptual figure (Figure 7) and contributed to Figure 1. All co-authors discussed the analysis, refined the methodology, and contributed to the text.

Competing interests. The contact author has declared that none of the authors has any competing interests.

395 *Acknowledgements.* We acknowledge the teams behind the RAPID-MOCHA-WBTS projects, Oleander Project, OSNAP program, AtlantOS project, and the Norwegian Institute of Marine Research for collecting and making data freely available. We thank David Smeed and Tom Rossby for kindly sharing updated records for the Western Boundary Current at 26.5^{o}N and the Oleander section, respectively. We also thank Kjell Arild Orvik and Algot Pedersen for sharing their knowledge about the Svinøy record and the most recent data. HLJ is grateful for funding from the NERC-NSF SNAP-DRAGON project (Grant NE/T013494/1).

400 References

Årthun, M., Eldevik, T., Viste, E., Drange, H., Furevik, T., Johnson, H. L., and Keenlyside, N. S.: Skillful prediction of northern climate provided by the ocean, Nature Communications, 8, https://doi.org/10.1038/ncomms15875, 2017.

Årthun, M., Asbjørnsen, H., Chafik, L., Johnson, H. L., and Våge, K.: Future strengthening of the Nordic Seas overturning circulation, Nature Communications, 14, 2065, https://doi.org/10.1038/s41467-023-37846-6, 2023.

405 Asbjørnsen, H. and Årthun, M.: Deconstructing Future AMOC Decline at 26.5°N, Geophysical Research Letters, 50, e2023GL103 515, https://doi.org/10.1029/2023GL103515, 2023.

Asbjørnsen, H., Årthun, M., Skagseth, Ø., and Eldevik, T.: Mechanisms of ocean heat anomalies in the Norwegian Sea, Journal of Geophysical Research: Oceans, 124, 2908–2923, https://doi.org/10.1029/2018JC014649, 2019.

Asbjørnsen, H., Johnson, H. L., and Årthun, M.: Variable Nordic Seas inflow linked to shifts in North Atlantic circulation, Journal of Climate, 410 34, 1–50, https://doi.org/10.1175/JCLI-D-20-0917.1, 2021.

Baehr, J., Keller, K., and Marotzke, J.: Detecting potential changes in the meridional overturning circulation at 26°N in the Atlantic, Climatic Change, 91, 11–27, https://doi.org/10.1007/s10584-006-9153-z, 2008.

Baringer, M. O. and Larsen, J. C.: Sixteen years of Florida Current Transport at 27° N, Geophysical Research Letters, 28, 3179–3182, https://doi.org/10.1029/2001GL013246, 2001.

415 Beadling, R. L., Russell, J. L., Stouffer, R. J., and Goodman, P. J.: Evaluation of Subtropical North Atlantic Ocean Circulation in CMIP5 Models against the Observational Array at 26.5°N and Its Changes under Continued Warming, Journal of Climate, 31, 9697–9718, https://doi.org/10.1175/JCLI-D-17-0845.1, 2018.

Berx, B., Hansen, B., Østerhus, S., Larsen, K. M., Sherwin, T., and Jochumsen, K.: Combining in situ measurements and altimetry to estimate volume, heat and salt transport variability through the Faroe-Shetland Channel, Ocean Science, 9, 639–654, https://doi.org/10.5194/os-9- 420 639-2013, 2013.

Bingham, R. J., Hughes, C. W., Roussenov, V., and Williams, R. G.: Meridional coherence of the North Atlantic meridional overturning circulation, Geophysical Research Letters, 34, L23 606, https://doi.org/10.1029/2007GL031731, 2007.

Brambilla, E., Talley, L. D., and Robbins, P. E.: Subpolar Mode Water in the northeastern Atlantic: 2. Origin and transformation, Journal of Geophysical Research, 113, C04 026, https://doi.org/10.1029/2006JC004063, 2008.

425 Bringedal, C., Eldevik, T., Skagseth, Ø., Spall, M. A., and Østerhus, S.: Structure and Forcing of Observed Exchanges across the Greenland-Scotland Ridge, Journal of Climate, 31, 9881–9901, https://doi.org/10.1175/JCLI-D-17-0889.1, 2018.

Caesar, L., Rahmstorf, S., Robinson, A., Feulner, G., and Saba, V.: Observed fingerprint of a weakening Atlantic Ocean overturning circulation, Nature, 556, 191–196, https://doi.org/10.1038/s41586-018-0006-5, 2018.

Caesar, L., McCarthy, G. D., Thornalley, D. J. R., Cahill, N., and Rahmstorf, S.: Current Atlantic Meridional Overturning Circulation weakest 430 in last millennium, Nature Geoscience, 14, 118–120, https://doi.org/10.1038/s41561-021-00699-z, 2021.

Caínzos, V., Hernández-Guerra, A., McCarthy, G. D., McDonagh, E. L., Armas, M. C., and Pérez-Hernández, M. D.: Thirty years of GO-SHIP and WOCE data: Atlantic Overturning of mass, heat and freshwater transport, Geophysical Research Letters, 49, e2021GL096 527, https://doi.org/10.1029/2021GL096527, 2022.

Chafik, L.: The response of the circulation in the Faroe-Shetland Channel to the North Atlantic Oscillation, Tellus, 64, 435 https://doi.org/10.3402/tellusa.v64i0.18423, 2012.

Chelton, D. B.: Effects of sampling errors in statistical estimation, Deep Sea Research Part A. Oceanographic Research Papers, 30, 1083–1103, https://doi.org/10.1016/0198-0149(83)90062-6, 1983.

Chi, L., Wolfe, C. L., and Hameed, S.: Reconsidering the Relationship Between Gulf Stream Transport and Dynamic Sea Level at U.S. East Coast, Geophysical Research Letters, 50, e2022GL102 018, https://doi.org/10.1029/2022GL102018, 2023.

440 Cunningham, S. A., Kanzow, T., Rayner, D., Baringer, M. O., Johns, W. E., Marotzke, J., Longworth, H. R., Grant, E. M., J-M Hirschi, J., Beal, L. M., Meinen, C. S., and Bryden, H. L.: Temporal Variability of the Atlantic Meridional Overturning Circulation at 26.5°N, Science, 317, 935–937, https://doi.org/10.1126/science.1141304, 2007.

Daniault, N., Mercier, H., Lherminier, P., Sarafanov, A., Falina, A., Zunino, P., Pérez, F. F., Ríos, A. F., Ferron, B., Huck, T., Thierry, V., and Gladyshev, S.: The northern North Atlantic Ocean mean circulation in the early 21st century, Progress in Oceanography, 146, 142–158, 445 https://doi.org/10.1016/J.POCEAN.2016.06.007, 2016.

Desbruyères, D., Chafik, L., and Maze, G.: A shift in the ocean circulation has warmed the subpolar North Atlantic Ocean since 2016, Communications Earth & Environment, 2, 48, https://doi.org/10.1038/s43247-021-00120-y, 2021.

Dong, S., Volkov, D. L., Goni, G., Pujiana, K., Tagklis, F., and Baringer, M.: Remote Impact of the Equatorial Pacific on Florida Current Transport, Geophysical Research Letters, 49, e2021GL096 944, https://doi.org/10.1029/2021GL096944, 2022.

450 Ebisuzaki, W.: A Method to Estimate the Statistical Significance of a Correlation When the Data Are Serially Correlated, Journal of Climate, 10, 2147–2153, https://doi.org/10.1175/1520-0442(1997)010<2147:AMTETS>2.0.CO;2, 1997.

ECCO Consortium, Fukumori, I., Wang, O., Fenty, I., Forget, G., Heimbach, P., and Ponte, R. M.: Synopsis of the ECCO Central Production Global Ocean and Sea-Ice State Estimate, Version 4 Release 4, Tech. rep., https://doi.org/10.5281/zenodo.3765928, 2021.

Eden, C. and Willebrand, J.: Mechanism of Interannual to Decadal Variability of the North Atlantic Circulation, Journal of Climate, 14, 455 2266–2280, https://doi.org/10.1175/1520-0442(2001)014<2266:MOITDV>2.0.CO;2, 2001.

Evans, D. G., Toole, J., Forget, G., Zika, J. D., Naveira Garabato, A. C., Nurser, A. J. G., and Yu, L.: Recent Wind-Driven Variability in Atlantic Water Mass Distribution and Meridional Overturning Circulation, Journal of Physical Oceanography, 47, 633–647, https://doi.org/10.1175/JPO-D-16-0089.1, 2017.

Flagg, C. N., Schwartze, G., Gottlieb, E., and Rossby, T.: Operating an Acoustic Doppler Current Profiler aboard a Container Vessel, in: 460 Journal of Atmospheric and Oceanic Technology, 15, 257–271, https://journals.ametsoc.org/view/journals/atot/15/1/1520-0426_1998_015_0257_oaadcp_2_0_co_2.xml, 1998.

Forget, G., Campin, J.-M., Heimbach, P., Hill, C. N., Ponte, R. M., and Wunsch, C.: ECCO version 4: an integrated framework for non-linear inverse modeling and global ocean state estimation, Geoscientific Model Development, 8, 3071–3104, https://doi.org/10.5194/gmd-8-3071-2015, 2015.

465 Fox, A. D., Handmann, P., Schmidt, C., Fraser, N., Rühs, S., Sanchez-Franks, A., Martin, T., Oltmanns, M., Johnson, C., Rath, W., Holliday, N. P., Biastoch, A., Cunningham, S. A., and Yashayaev, I.: Exceptional freshening and cooling in the eastern subpolar North Atlantic caused by reduced Labrador Sea surface heat loss, Ocean Science, 18, 1507–1533, https://doi.org/10.5194/os-18-1507-2022, 2022.

Frajka-Williams, E., Ansorge, I. J., Baehr, J., Bryden, H. L., Chidichimo, M. P., Cunningham, S. A., Danabasoglu, G., Dong, S., Donohue, K. A., Elipot, S., Heimbach, P., Holliday, N. P., Hummels, R., Jackson, L. C., Karstensen, J., Lankhorst, M., Le Bras, I. A., Lozier, M. S., 470 McDonagh, E. L., Meinen, C. S., Mercier, H., Moat, B. I., Perez, R. C., Piecuch, C. G., Rhein, M., Srokosz, M. A., Trenberth, K. E., Bacon, S., Forget, G., Goni, G., Kieke, D., Koelling, J., Lamont, T., McCarthy, G. D., Mertens, C., Send, U., Smeed, D. A., Speich, S., van den Berg, M., Volkov, D., and Wilson, C.: Atlantic Meridional Overturning Circulation: Observed Transport and Variability, Frontiers in Marine Science, 6, 260, https://doi.org/10.3389/fmars.2019.00260, 2019.

Frajka-Williams, E., Foukal, N., and Danabasoglu, G.: Should AMOC observations continue: how and why?, Philosophical Transactions of the Royal Society A, 381, https://doi.org/10.1098/RSTA.2022.0195, 2023.

Frajka-Williams, E., Johns, W. E., Meinen, C. S., Beal, L. M., and Cunningham, S. A.: Eddy impacts on the Florida Current, Geophysical Research Letters, 40, 349–353, https://doi.org/10.1002/grl.50115, 2013.

Fraser, N. J. and Cunningham, S. A.: 120 years of AMOC variability reconstructed from observations using the Bernoulli inverse, Geophysical Research Letters, 48, e2021GL093 893, https://doi.org/10.1029/2021GL093893, 2021.

Fu, Y., Li, F., Karstensen, J., and Wang, C.: A stable Atlantic Meridional Overturning Circulation in a changing North Atlantic Ocean since the 1990s, Science Advances, 6, 7836–7863, http://advances.sciencemag.org/, 2020.

Fu, Y., Lozier, M. S., Biló, T. C., Bower, A. S., Cunningham, S. A., Cyr, F., de Jong, M. F., deYoung, B., Drysdale, L., Fraser, N., Fried, N., Furey, H. H., Han, G., Handmann, P., Holliday, N. P., Holte, J., Inall, M. E., Johns, W. E., Jones, S., Karstensen, J., Li, F., Pacini, A., Pickart, R. S., Rayner, D., Straneo, F., and Yashayaev, I.: Seasonality of the Meridional Overturning Circulation in the subpolar North Atlantic, Communications Earth & Environment, 4, 181, https://doi.org/10.1038/s43247-023-00848-9, 2023.

Gu, S., Liu, Z., and Wu, L.: Time Scale Dependence of the Meridional Coherence of the Atlantic Meridional Overturning Circulation, Journal of Geophysical Research: Oceans, 125, e2019JC015 838, https://doi.org/10.1029/2019JC015838, 2020.

Hamed, K. H. and Rao, R. A.: A modified Mann-Kendall trend test for autocorrelated data, Journal of Hydrology, 204, 182–196, https://doi.org/10.1016/S0022-1694(97)00125-X, 1997.

Hameed, S., Wolfe, C. L. P., and Chi, L.: Icelandic Low and Azores High Migrations Impact Florida Current Transport in Winter, Journal of Physical Oceanography, 51, 3135–3147, https://doi.org/10.1175/JPO-D-20-0108.1, 2021.

Han, L.: Exploring the AMOC Connectivity Between the RAPID and OSNAP Lines With a Model-Based Data Set, Geophysical Research Letters, 50, e2023GL105 225, https://doi.org/10.1029/2023GL105225, 2023.

Hansen, B., Larsen, K. M. H., Hátún, H., Kristiansen, R., Mortensen, E., and Østerhus, S.: Transport of volume, heat, and salt towards the Arctic in the Faroe Current 1993-2013, Ocean Sci, 11, 743–757, https://doi.org/10.5194/os-11-743-2015, 2015.

Hansen, B., Margretha, K., Larsen, H., Hátún, H., and Østerhus, S.: A stable Faroe Bank Channel overflow 1995-2015, Ocean Sci, 12, 1205–1220, https://doi.org/10.5194/os-12-1205-2016, 2016.

Heimbach, P., Hill, C., and Giering, R.: An efficient exact adjoint of the parallel MIT General Circulation Model, generated via automatic differentiation, Future Generation Computer Systems, 21, 1356–1371, https://doi.org/10.1016/J.FUTURE.2004.11.010, 2005.

Hersbach, H., Bell, B., Berrisford, P., Hirahara, S., Horányi, A., Muñoz-Sabater, J., Nicolas, J., Peubey, C., Radu, R., Schepers, D., Simmons, A., Soci, C., Abdalla, S., Abellan, X., Balsamo, G., Bechtold, P., Biavati, G., Bidlot, J., Bonavita, M., Chiara, G., Dahlgren, P., Dee, D., Diamantakis, M., Dragani, R., Flemming, J., Forbes, R., Fuentes, M., Geer, A., Haimberger, L., Healy, S., Hogan, R. J., Hólm, E., Janisková, M., Keeley, S., Laloyaux, P., Lopez, P., Lupu, C., Radnoti, G., Rosnay, P., Rozum, I., Vamborg, F., Villaume, S., and Thépaut, J.: The ERA5 global reanalysis, Quarterly Journal of the Royal Meteorological Society, 146, 1999–2049, https://doi.org/10.1002/qj.3803, 2020.

Hirschi, J. J.-M., Frajka-Williams, E., Blaker, A. T., Sinha, B., Coward, A., Hyder, P., Biastoch, A., Böning, C., Barnier, B., Penduff, T., Garcia, I., Fransner, F., and Madec, G.: Loop Current Variability as Trigger of Coherent Gulf Stream Transport Anomalies, Journal of Physical Oceanography, 49, 2115–2132, https://doi.org/10.1175/JPO-D-18-0236.1, 2019.

Hogg, N. G.: On the transport of the Gulf Stream between Cape Hatteras and the Grand Banks, Deep Sea Research Part A. Oceanographic Research Papers, 39, 1231–1246, https://doi.org/10.1016/0198-0149(92)90066-3, 1992.

Ingvaldsen, R. B., Loeng, H., and Asplin, L.: Variability in the Atlantic inflow to the Barents Sea based on a one-year time series from moored current meters, Continental Shelf Research, 22, 505–519, https://doi.org/10.1016/S0278-4343(01)00070-X, 2002.

Ingvaldsen, R. B., Asplin, L., and Loeng, H.: Velocity field of the western entrance to the Barents Sea, Journal of Geophysical Research: Oceans, 109, C03 021, https://doi.org/10.1029/2003JC001811, 2004.

515 Jackson, L. C., Biastoch, A., Buckley, M. W., Desbruyères, D. G., Frajka-Williams, E., Moat, B., and Robson, J.: The evolution of the North Atlantic Meridional Overturning Circulation since 1980, Nature Reviews Earth & Environment, 3, 241–254, https://doi.org/10.1038/s43017-022-00263-2, 2022.

Jochumsen, K., Moritz, M., Nunes, N., Quadfasel, D., Larsen, K. M., Hansen, B., Valdimarsson, H., and Jonsson, S.: Revised transport estimates of the Denmark Strait overflow, Journal of Geophysical Research: Oceans, 122, 3434–3450, https://doi.org/10.1002/2017JC012803,

520 2017.

Johnson, H. L. and Marshall, D. P.: A Theory for the Surface Atlantic Response to Thermohaline Variability, Journal of Physical Oceanography, 32, 1121–1132, https://doi.org/10.1175/1520-0485(2002)032<1121:ATFTSA>2.0.CO;2, 2002.

Jónsson, S. and Valdimarsson, H.: Water mass transport variability to the North Icelandic shelf, 1994–2010, ICES Journal of Marine Science, 69, 809–815, https://doi.org/10.1093/icesjms/fss024, 2012.

525 Keenlyside, N. S., Latif, M., Jungclaus, J., Kornblueh, L., and Roeckner, E.: Advancing decadal-scale climate prediction in the North Atlantic sector, Nature Geoscience, 453, 84–88, https://doi.org/10.1038/nature06921, 2008.

Kelson, R. L., Straub, D. N., and Dufour, C. O.: Using CMIP6 models to assess the significance of the observed trend in the Atlantic Meridional Overturning Circulation, Geophysical Research Letters49, 49, e2022GL100 202, https://doi.org/10.1029/2022GL100202, 2022.

Kilbourne, K. H., Wanamaker, A. D., Moffa-Sanchez, P., Reynolds, D. J., Amrhein, D. E., Butler, P. G., Gebbie, G., Goes, M., Jansen, M. F.,

530 Little, C. M., Mette, M., Moreno-Chamarro, E., Ortega, P., Otto-Bliesner, B. L., Rossby, T., Scourse, J., and Whitney, N. M.: Atlantic circulation change still uncertain, Nature Geoscience, 15, 165–167, https://doi.org/10.1038/s41561-022-00896-4, 2022.

Kostov, Y., Johnson, H. L., Marshall, D. P., Heimbach, P., Forget, G., Holliday, N. P., Lozier, M. S., Li, F., Pillar, H. R., and Smith, T.: Distinct sources of interannual subtropical and subpolar Atlantic overturning variability, Nature Geoscience, 14, 491–495, https://doi.org/10.1038/s41561-021-00759-4, 2021.

535 Koul, V., Tesdal, J.-E., Bersch, M., Hátún, H., Brune, S., Borchert, L., Haak, H., Schrum, C., and Baehr, J.: Unraveling the choice of the north Atlantic subpolar gyre index, Scientific Reports, 10, 1005, https://doi.org/10.1038/s41598-020-57790-5, 2020.

Kwon, Y.-O., Alexander, M. A., Bond, N. A., Frankignoul, C., Nakamura, H., Qiu, B., and Thompson, L. A.: Role of the Gulf Stream and Kuroshio–Oyashio Systems in Large-Scale Atmosphere–Ocean Interaction: A Review, Journal of Climate, 23, 3249–3281, https://doi.org/10.1175/2010JCLI3343.1, 2010.

540 Larsen, J. C. and Sanford, T. B.: Florida Current Volume Transports from Voltage Measurements, Science, 227, 302–304, https://doi.org/10.1126/science.227.4684.302, 1985.

Li, F., Lozier, M. S., and Johns, W. E.: Calculating the Meridional Volume, Heat, and Freshwater Transports from an Observing System in the Subpolar North Atlantic: Observing System Simulation Experiment, Journal of Atmospheric and Oceanic Technology, 34, 1483–1500, https://doi.org/10.1175/JTECH-D-16-0247.1, 2017.

545 Lique, C. and Thomas, M. D.: Latitudinal shift of the Atlantic Meridional Overturning Circulation source regions under a warming climate, Nature Climate Change, 8, 1013–1020, https://doi.org/10.1038/s41558-018-0316-5, 2018.

Lobelle, D., Beaulieu, C., Livina, V., Sévellec, F., and Frajka-Williams, E.: Detectability of an AMOC Decline in Current and Projected Climate Changes, Geophysical Research Letters, 47, e2020GL089 974, https://doi.org/10.1029/2020GL089974, 2020.

Lozier, M. S.: Deconstructing the Conveyor Belt, Science, 328, 1507–1511, https://doi.org/10.1126/science.1189250, 2010.

550 Lozier, M. S.: Overturning in the North Atlantic, Annual Review of Marine Science, 4, 291–315, https://doi.org/10.1146/annurev-marine-120710-100740, 2012.

Lozier, M. S., Roussenov, V., Reed, M. S. C., and Williams, R. G.: Opposing decadal changes for the North Atlantic meridional overturning circulation, Nature Geoscience, 3, 728–734, https://doi.org/10.1038/ngeo947, 2010.

Lozier, S., Bacon, S., Bower, A. S., Cunningham, S. A., Femke de Jong, M., de Steur, L., deYoung, B., Fischer, J., Gary, S. F., Greenan, B.

555 J. W., Heimbach, P., Holliday, N. P., Houpert, L., Inall, M. E., Johns, W. E., Johnson, H. L., Karstensen, J., Li, F., Lin, X., Mackay, N., Marshall, D. P., Mercier, H., Myers, P. G., Pickart, R. S., Pillar, H. R., Straneo, F., Thierry, V., Weller, R. A., Williams, R. G., Wilson, C., Yang, J., Zhao, J., and Zika, J. D.: Overturning in the Subpolar North Atlantic Program: A New International Ocean Observing System, Bulletin of the American Meteorological Society, 98, 737–752, https://doi.org/10.1175/BAMS-D-16-0057.1, 2017.

Manabe, S. and Stouffer, R. J.: Multiple-Century Response of a Coupled Ocean-Atmosphere Model to an Increase of Atmospheric Carbon

560 Dioxide, Journal of Climate, 7, 5–23, https://doi.org/10.1175/1520-0442(1994)007<0005:MCROAC>2.0.CO;2, 1994.

Mann, C.: The termination of the Gulf Stream and the beginning of the North Atlantic Current, Deep Sea Research and Oceanographic Abstracts, 14, 337–359, https://doi.org/10.1016/0011-7471(67)90077-0, 1967.

Marshall, Johnson, H., and Goodman, J.: A Study of the Interaction of the North Atlantic Oscillation with Ocean Circulation, Journal of Climate, 14, 1399–1421, https://doi.org/10.1175/1520-0442(2001)014<1399:ASOTIO>2.0.CO;2, 2001.

565 Marshall, D. P. and Johnson, H. L.: Propagation of Meridional Circulation Anomalies along Western and Eastern Boundaries, Journal of Physical Oceanography, 43, 2699–2717, https://doi.org/10.1175/JPO-D-13-0134.1, 2013.

Mauritzen, C.: Production of dense overflow waters feeding the North Atlantic across the Greenland-Scotland Ridge. Part 1: Evidence for a revised circulation scheme, Deep Sea Research Part I: Oceanographic Research Papers, 43, 769–806, https://doi.org/10.1016/0967-0637(96)00037-4, 1996.

570 McCarthy, G. D., Smeed, D. A., Johns, W. E., Frajka-Williams, E., Moat, B. I., Rayner, D., Baringer, M. O., Meinen, C. S., Collins, J., and Bryden, H.: Measuring the Atlantic Meridional Overturning Circulation at 26°N, Progress in Oceanography, 130, 91–111, https://doi.org/10.1016/J.POCEAN.2014.10.006, 2015.

Meinen, C. S. and Watts, D. R.: Vertical structure and transport on a transect across the North Atlantic Current near 42°N: Time series and mean, Journal of Geophysical Research: Oceans, 105, 21 869–21 891, https://doi.org/10.1029/2000JC900097, 2000.

575 Meinen, C. S., Baringer, M. O., and Garcia, R. F.: Florida Current transport variability: An analysis of annual and longer-period signals, Deep Sea Research Part I: Oceanographic Research Papers, 57, 835–846, https://doi.org/10.1016/J.DSR.2010.04.001, 2010.

Meinen, C. S., Johns, W. E., Moat, B. I., Smith, R. H., Johns, E. M., Rayner, D., Frajka-Williams, E., Garcia, R. F., and Garzoli, S. L.: Structure and Variability of the Antilles Current at 26.5°N, Journal of Geophysical Research: Oceans, 124, 3700–3723, https://doi.org/10.1029/2018JC014836, 2019.

580 Mercier, H., Lherminier, P., Sarafanov, A., Gaillard, F., Daniault, N., Desbruyères, D., Falina, A., Ferron, B., Gourcuff, C., Huck, T., and Thierry, V.: Variability of the meridional overturning circulation at the Greenland–Portugal OVIDE section from 1993 to 2010, Progress in Oceanography, 132, 250–261, https://doi.org/10.1016/J.POCEAN.2013.11.001, 2015.

Mielke, C., Frajka-Williams, E., and Baehr, J.: Observed and simulated variability of the AMOC at 26°N and 41°N, Geophysical Research Letters, 40, 1159–1164, https://doi.org/10.1002/grl.50233, 2013.

585 Moat, B. I., Smeed, D. A., Frajka-Williams, E., Desbruyères, D. G., Beaulieu, C., Johns, W. E., Rayner, D., Sanchez-Franks, A., Baringer, M. O., Volkov, D., Jackson, L. C., and Bryden, H. L.: Pending recovery in the strength of the meridional overturning circulation at 26N, Ocean Science, 16, 863–874, https://doi.org/10.5194/os-16-863-2020, 2020.

Moat, B. I., Frajka-Williams, E., Rayner, D., Johns, W. E., Baringer, M. O., Volkov, D. L., and Collins, J.: Atlantic meridional overturning circulation observed by the RAPID-MOCHA-WBTS array at 26N from 2004 to 2020 (v2020.2), NERC EDS British Oceanographic Data 590 Centre NOC [data set], https://doi.org/10.5285/e91b10af-6f0a-7fa7-e053-6c86abc05a09, 2022.

Moffa-Sánchez, P., Moreno-Chamarro, E., Reynolds, D. J., Ortega, P., Cunningham, L., Swingedouw, D., Amrhein, D. E., Halfar, J., Jonkers, L., Jungclaus, J. H., Perner, K., Wanamaker, A., and Yeager, S.: Variability in the Northern North Atlantic and Arctic Oceans Across the Last Two Millennia: A Review, Paleoceanography and Paleoclimatology, 34, 1399–1436, https://doi.org/10.1029/2018PA003508, 2019.

Orvik, K. A.: Long-Term Moored Current and Temperature Measurements of the Atlantic Inflow Into the Nordic Seas in the Norwegian 595 Atlantic Current; 1995–2020, Geophysical Research Letters, 49, e2021GL096 427, https://doi.org/10.1029/2021GL096427, 2022.

Orvik, K. A. and Skagseth, Ø.: Monitoring the Norwegian Atlantic slope current using a single moored current meter, Continental Shelf Research, 23, 159–176, https://doi.org/10.1016/S0278-4343(02)00172-3, 2003a.

Orvik, K. A. and Skagseth, Ø.: The impact of the wind stress curl in the North Atlantic on the Atlantic inflow to the Norwegian Sea toward the Arctic, Geophysical Research Letters, 30, https://doi.org/10.1029/2003GL017932, 2003b.

600 Østerhus, S., Woodgate, R., Valdimarsson, H., Turrell, B., de Steur, L., Quadfasel, D., Olsen, S. M., Moritz, M., Lee, C. M., Larsen, K. M. H., Jónsson, S., Johnson, C., Jochumsen, K., Hansen, B., Curry, B., Cunningham, S., and Berx, B.: Arctic Mediterranean Exchanges: A consistent volume budget and trends in transports from two decades of observations, Ocean Science, 15, 379–399, https://doi.org/10.5194/os-15-379-2019, 2019.

Palter, J. B.: The Role of the Gulf Stream in European Climate, Annual Review of Marine Science, 7, 113–137, 605 https://doi.org/10.1146/annurev-marine-010814-015656, 2015.

Piecuch, C. G.: Likely weakening of the Florida Current during the past century revealed by sea-level observations, Nature Communications, 11, 3973, https://doi.org/10.1038/s41467-020-17761-w, 2020.

Piecuch, C. G. and Beal, L. M.: Robust Weakening of the Gulf Stream During the Past Four Decades Observed in the Florida Straits, Geophysical Research Letters, 50, e2023GL105 170, https://doi.org/10.1029/2023GL105170, 2023.

610 Piecuch, C. G., Ponte, R. M., Little, C. M., Buckley, M. W., and Fukumori, I.: Mechanisms underlying recent decadal changes in subpolar North Atlantic Ocean heat content, Journal of Geophysical Research: Oceans, 122, 7181–7197, https://doi.org/10.1002/2017JC012845, 2017.

Polyakov, I. V., Ingvaldsen, R. B., Pnyushkov, A. V., Bhatt, U. S., Francis, J. A., Janout, M., Kwok, R., and Skagseth, Ø.: Fluctuating Atlantic inflows modulate Arctic atlantification, Science, 381, 972–979, https://doi.org/10.1126/science.adh5158, 2023.

615 Rhein, M., Mertens, C., and Roessler, A.: Observed Transport Decline at 47°N, Western Atlantic, Journal of Geophysical Research: Oceans, 124, 4875–4890, https://doi.org/10.1029/2019JC014993, 2019.

Richter, K., Furevik, T., and Orvik, K. A.: Effect of wintertime low-pressure systems on the Atlantic inflow to the Nordic seas, Journal of Geophysical Research, 114, C09 006, https://doi.org/10.1029/2009JC005392, 2009.

Roberts, C. D., Waters, J., Peterson, K. A., Palmer, M. D., McCarthy, G. D., Frajka-Williams, E., Haines, K., Lea, D. J., Martin, M. J., Storkey, 620 D., Blockley, E. W., and Zuo, H.: Atmosphere drives recent interannual variability of the Atlantic meridional overturning circulation at 26.5°N, Geophysical Research Letters, 40, 5164–5170, https://doi.org/10.1002/grl.50930, 2013.

Roessler, A., Rhein, M., Kieke, D., and Mertens, C.: Long-term observations of North Atlantic Current transport at the gateway between western and eastern Atlantic, Journal of Geophysical Research: Oceans, 120, 4003–4027, https://doi.org/10.1002/2014JC010662, 2015.

Roquet, F. and Wunsch, C.: The Atlantic Meridional Overturning Circulation and its Hypothetical Collapse, Tellus A: Dynamic Meteorology and Oceanography, 74, 393–398, https://doi.org/10.16993/tellusa.679, 2022.

Rossby, T., Flagg, C. N., and Donohue, K.: Interannual variations in upper-ocean transport by the Gulf Stream and adjacent waters between New Jersey and Bermuda, Journal of Marine Research, 63, 203–226, https://elischolar.library.yale.edu/journal_of_marine_research/77, 2005.

Rossby, T., Flagg, C. N., Donohue, K., Sanchez-Franks, A., and Lillibridge, J.: On the long-term stability of Gulf Stream transport based on 20 years of direct measurements, Geophysical Research Letters, 41, 114–120, https://doi.org/10.1002/2013GL058636, 2014.

Rossby, T., Flagg, C., Dohan, K., Fontana, S., Curry, R., Andres, M., and Forsyth, J.: Oleander is More than a Flower: Twenty-Five Years of Oceanography Aboard a Merchant Vessel, Oceanography, 32, 126–137, https://doi.org/10.5670/oceanog.2019.319, 2019.

Rossby, T., Chafik, L., and Houpert, L.: What can Hydrography Tell Us about the strength of the Nordic Seas MOC over the last 70 to 100 years?, Geophysical Research Letters, 47, e2020GL087 456, https://doi.org/10.1029/2020GL087456, 2020.

Sanchez-Franks, A., Flagg, C., and Rossby, T.: A comparison of transport and position between the Gulf Stream east of Cape Hatteras and the Florida Current, Journal of Marine Research, 72, https://elischolar.library.yale.edu/journal_of_marine_research/394, 2014.

Sanchez-Franks, A., Hameed, S., and Wilson, R. E.: The Icelandic Low as a Predictor of the Gulf Stream North Wall Position, Journal of Physical Oceanography, 46, 817–826, https://doi.org/10.1175/JPO-D-14-0244.1, 2016.

Sanders, R. N. C., Jones, D. C., Josey, S. A., Sinha, B., and Forget, G.: Causes of the 2015 North Atlantic cold anomaly in a global state estimate, Ocean Science, 18, 953–978, https://doi.org/10.5194/os-18-953-2022, 2022.

Sarafanov, A.: On the effect of the North Atlantic Oscillation on temperature and salinity of the subpolar North Atlantic intermediate and deep waters, ICES Journal of Marine Science, 66, 1448–1454, https://doi.org/10.1093/icesjms/fsp094, 2009.

Sen Gupta, A., Stellema, A., Pontes, G. M., Taschetto, A. S., Vergés, A., and Rossi, V.: Future changes to the upper ocean Western Boundary Currents across two generations of climate models, Scientific Reports, 11, 9538, https://doi.org/10.1038/s41598-021-88934-w, 2021.

Skagseth, Ø. and Orvik, K. A.: Identifying fluctuations in the Norwegian Atlantic Slope Current by means of empirical orthogonal functions, Continental Shelf Research, 22, 547–563, https://doi.org/10.1016/S0278-4343(01)00086-3, 2002.

Smeed, D. A., Josey, S. A., Beaulieu, C., Johns, W. E., Moat, B. I., Frajka-Williams, E., Rayner, D., Meinen, C. S., Baringer, M. O., Bryden, H. L., and McCarthy, G. D.: The North Atlantic Ocean Is in a State of Reduced Overturning, Geophysical Research Letters, 45, 1527–1533, https://doi.org/10.1002/2017GL076350, 2018.

Tesdal, J. and Haine, T. W. N.: Dominant terms in the freshwater and heat budgets of the subpolar North Atlantic Ocean and Nordic Seas from 1992 to 2015, Journal of Geophysical Research: Oceans, 125, e2020JC016 435, https://doi.org/10.1029/2020JC016435, 2020.

Thornalley, D. J. R., Oppo, D. W., Ortega, P., Robson, J. I., Brierley, C. M., Davis, R., Hall, I. R., Moffa-Sanchez, P., Rose, N. L., Spooner, P. T., Yashayaev, I., and Keigwin, L. D.: Anomalously weak Labrador Sea convection and Atlantic overturning during the past 150 years, Nature, 556, 227–230, https://doi.org/10.1038/s41586-018-0007-4, 2018.

Weijer, W., Cheng, W., Garuba, O. A., Hu, A., and Nadiga, B. T.: CMIP6 Models Predict Significant 21st Century Decline of the Atlantic Meridional Overturning Circulation, Geophysical Research Letters, 47, e2019GL086 075, https://doi.org/10.1029/2019GL086075, 2020.

Worthington, E. L., Moat, B. I., Smeed, D. A., Mecking, J. V., Marsh, R., and Mccarthy, G. D.: A 30-year reconstruction of the Atlantic meridional overturning circulation shows no decline, Ocean Science, 17, 285–299, https://doi.org/10.5194/os-17-285-2021, 2021.

Wunsch, C. and Heimbach, P.: Two Decades of the Atlantic Meridional Overturning Circulation: Anatomy, Variations, Extremes, Prediction, and Overcoming Its Limitations, Journal of Climate, 26, 7167–7186, https://doi.org/10.1175/JCLI-D-12-00478.1, 2013.

Zhang, R.: Latitudinal dependence of Atlantic meridional overturning circulation (AMOC) variations, Geophysical Research Letters, 37, L16 703, https://doi.org/10.1029/2010GL044474, 2010.

Zhang, R., Sutton, R., Danabasoglu, G., Kwon, Y. O., Marsh, R., Yeager, S. G., Amrhein, D. E., and Little, C. M.: A Review of the Role of the Atlantic Meridional Overturning Circulation in Atlantic Multidecadal Variability and Associated Climate Impacts, Reviews of Geophysics, 57, 316–375, https://doi.org/10.1029/2019RG000644, 2019.

Zhao, J. and Johns, W.: Wind-forced interannual variability of the Atlantic Meridional Overturning Circulation at 26.5°N, Journal of Geophysical Research: Oceans, 119, 2403–2419, https://doi.org/10.1002/2013JC009407, 2014.

Zou, S., Lozier, M. S., and Xu, X.: Latitudinal Structure of the Meridional Overturning Circulation Variability on Interannual to Decadal Time Scales in the North Atlantic Ocean, Journal of Climate, 33, 3845–3862, https://doi.org/10.1175/JCLI-D-19-0215.1, 2020.